

International Conference on the

PHYSICS OF TRANSITION METALS

Volume I

Darmstadt, Germany

July 20 - 24, 1992

Editors

P M Oppeneer

J Kübler

				<i>Sc</i>	<i>Ti</i>	<i>V</i>	
				<i>Cr</i>	<i>Mn</i>	<i>Fe</i>	<i>Co</i>
			<i>Ni</i>	<i>Y</i>	<i>Zr</i>	<i>Nb</i>	<i>Mo</i>
		<i>Tc</i>	<i>Ru</i>	<i>Rh</i>	<i>Pd</i>	<i>La</i>	<i>Hf</i>
	<i>Ta</i>	<i>W</i>	<i>Re</i>	<i>Os</i>	<i>Ir</i>	<i>Pt</i>	<i>Ac</i>

World Scientific

CONNECTION BETWEEN GIANT MAGNETORESISTANCE AND ROUGHNESS IN SPUTTERED Fe/Cr SUPERLATTICES

DAVID M. KELLY*, ERIC E. FULLERTON*, F.T. PARKER**, J. GUIMPEL*,
Y. BRUYNSERAEDE†, and IVAN K. SCHULLER*

*Dept. of Physics, University of California, San Diego, La Jolla, Ca 92093-0319, USA

** Center for Magnetic Recording, University of California, San Diego, La Jolla, Ca 92093, USA

†Laboratorium voor Vaste Stof-Fysika en Magnetisme, Katholieke Universiteit Leuven
B-3001 Leuven, Belgium

Detailed structural, magnetotransport, magnetization and Mössbauer measurements of sputtered Fe/Cr superlattices are presented. The interfacial roughness of the superlattice can be controlled systematically and reproducibly by sputtering at different Ar pressures. Conversion electron Mössbauer spectroscopy results indicate that the amount of interdiffusion remains constant in the films as the interfacial roughness increases. The results show that roughness enhances the magnetoresistance for all Cr thickness in the range of 10 to 40 Å.

The observation of giant magnetoresistance (GMR) in Fe/Cr superlattices¹ has stimulated a great deal of experimental and theoretical work.²⁻¹¹ The GMR has been attributed to spin dependent scattering of the conduction electrons^{3,6-11} in the antiferromagnetically coupled layers.¹² It has been experimentally determined that the spin dependent scattering is indeed occurring at the magnetic-nonmagnetic interface of Fe/Cr.¹³ Other work suggests that spin dependent scattering also occurs in the bulk for Ni, Co and NiFe/Cu exchange biased trilayers.¹⁴ The exchange biased trilayers directly demonstrated that the angle between the magnetizations in adjacent magnetic layers is the important controlling parameter of the GMR effect,¹⁵ and GMR has even been observed in heterogeneous Co-Cu alloys indicating that a superlattice is not necessary.^{16,17} Petroff et al.¹⁸ have demonstrated that there is an optimal amount of intermixing of Fe and Cr at the interfaces for which the maximum GMR develops, and increasing the interdiffusion throughout these multilayers increases the resistivity and decreases the GMR. The nature of the interface, interdiffusion between the Fe and Cr layers and the way in which the GMR is affected by these changes are therefore of great interest.

In this work, we have systematically varied the roughness of the interfaces in sputtered Fe/Cr superlattices by changing the Ar sputtering gas pressure. These structural changes are clearly evident in the low angle x-ray spectra, showing that films sputtered at high pressure are considerably rougher than those sputtered at low pressure. We present conversion electron Mössbauer spectroscopy (CEMS) data which indicates that roughening the interfaces in this fashion leads to no significant changes in the amount of interdiffusion present in the films. In contrast to the work done on MBE grown samples,¹⁸ we have not intermixed the Fe and Cr at the interface, we have simply made the position of the interface more random. Magnetization data show that the remanent magnetization increases in the rougher films, indicating that the ferromagnetically coupled regions increase with roughness, as expected. In spite of this, the GMR increases substantially with increasing interfacial roughness. Interfacial roughness is therefore a crucial parameter controlling the GMR, must be included in any theoretical treatment of GMR, and must be critically examined in any experimental work on Fe/Cr superlattices.

Fe/Cr superlattices were prepared by dc magnetron sputtering system at a base pressure less than 5×10^{-7} Torr on ambient temperature Si and sapphire substrates using a computer controlled rotating platform.¹⁹ The Fe and Cr guns were carefully shielded to avoid cross talk, and we chose not to use shutters which may lead to instabilities in the plasma giving rise to fluctuations in the growth rate on the substrates. All films in this study were grown at the same rate, as measured by quartz crystal rate monitors located near the substrates. Only the sputtering pressure was varied, minimizing the effects due to changes in other deposition parameters. In this fashion, we are able to systematically control the interfacial roughness of

the films. We have shown that many other deposition parameters affect the interfacial roughness,²⁰ however we will discuss only the effect of changing the Ar pressure.

The structure of the films was characterized by both low and high angle x-ray diffraction with a Rigaku RU200 diffractometer using $\text{CuK}\alpha$ radiation. The low angle spectra contain information on the interfacial structure of the superlattice, and the high angle spectra provide information about the disorder in the superlattice on the atomic scale. Examination of the low angle spectra clearly show the differences in roughness in samples of the same thickness and modulation. High angle data, on the other hand, can be used to identify changes in the grain size and mosaic spread of the superlattices. Structural refinement techniques have proved successful at fitting high angle x-ray spectra in a variety of metallic superlattices,²¹ however Fe/Cr poses some difficulties. Fe and Cr are nearly identical in lattice spacing and scattering power which conspire to give a high angle spectra with few features. Thus, we will not present any high angle x-ray refinements for this system.

The magnetotransport data were taken in a superconducting magnet system designed for low temperature transport measurement. For this work, all data were taken at 4.2K on photolithographically patterned films using standard 4-probe DC methods. The 10K magnetization was measured with a Quantum Design SQUID magnetometer in fields up to 5 Tesla.

Additionally, the local environment of the Fe atoms was probed by CEMS. Fits to the CEMS spectra yield a distribution of the hyperfine fields $P(H_N)$ at the Fe nuclei. Since the hyperfine field of the Fe nuclei is sensitive to the number of Cr nearest and next nearest neighbors, this technique allows for a measure of the interdiffusion of Cr and Fe. This technique has proven quite successful in other systems.²²

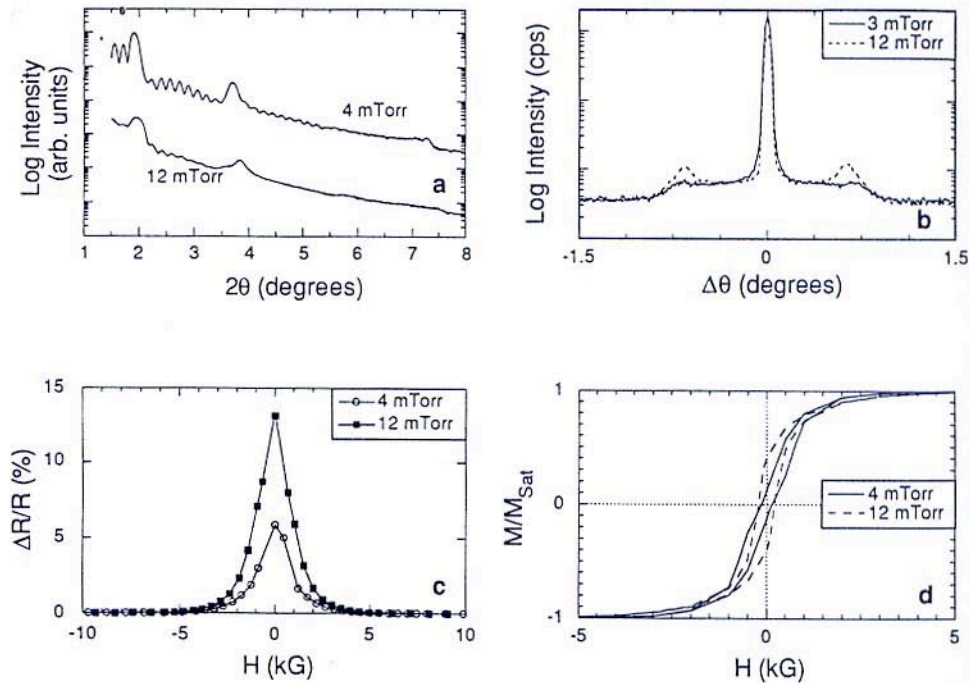


Figure 1: (a) Low angle x-ray scans for $[\text{Fe}(30\text{\AA})/\text{Cr}(18\text{\AA})]_{10}$ superlattices sputtered at 4 and 12 mTorr (spectra were offset for clarity), (b) rocking curves, (c) magnetoresistance at 4.2K, and (d) hysteresis loops at 10K for the same samples.

Fig. 1a shows typical θ - 2θ low angle x-ray spectra for $[\text{Fe}(30\text{\AA})/\text{Cr}(18\text{\AA})]_{10}$ films grown at 4 and 12 mTorr. The intensities have been offset for clarity. These films were grown consecutively, thus minimizing the possibility of other sputtering parameters changing from sample to sample. The spectra are made up of two parts, a high frequency component arising from the finite thickness of the multilayer ("finite size peaks"), the other lower frequency part from the periodicity of the superlattice ("Bragg peaks"). The 4 mTorr sample shows Bragg peaks up to fourth order, the third order peak being suppressed as the ratio of Fe to Cr is almost 2:1. The 12 mTorr sample shows broader Bragg peaks of lower intensity, and exhibits almost no fourth order peak. In addition, the 4 mTorr sample exhibits clear finite size peaks beyond the third Bragg peak, whereas the 12 mTorr sample has no finite size peaks evident beyond the second order Bragg peak. The broadening of the Bragg peaks and loss of finite size peaks have been seen in other systems and are characteristic of rougher interfaces.^{23,24}

Fig. 1b shows the low angle rocking curves taken at the 2θ position of the first order Bragg peak for the samples in fig. 1a. The central peak, resulting from the specular reflectivity, is only slightly broadened, however the intensity is significantly reduced. The intensity lost to the specular beam appears out in the wings of the pattern as increased diffuse scattering. This is clear evidence of increasing roughness.²⁵ The conclusion that can be drawn from figs. 1a,b is that with increasing sputtering pressure, the interfacial roughness of the superlattices increases. Similar results have been observed in systems studied for application as x-ray mirrors where increased sputtering pressure also gives rougher layers.²⁶

Fig. 1c shows the magnetoresistance of the same films measured at 4.2K. The films were saturated at 10kG, then the field was swept to -10kG. The GMR is defined in the usual fashion, where $\Delta R/R$ (or, equivalently, $\Delta\rho/\rho$ where ρ is the resistivity) equals the resistance at an applied field H minus the resistance of the film when saturated (the resistance at 10 kG for all the films in this study), divided by the saturation resistance. As the films become rougher, the $\Delta R/R$ increases dramatically. The saturation resistivities are almost unaffected by the increasing roughness for the 10 bilayer films, therefore it is clear that the saturation resistivity of these films is not dominated by interfacial scattering and that the changes in $\Delta R/R$ are due to changes in $\Delta\rho$. This is in agreement with results from MBE grown samples¹⁸ in which smoother samples had smaller magnetoresistance.

Shown in fig. 1d are hysteresis loops for the 4 and 12 mTorr samples. The data are normalized to the saturation magnetization values, which were both about 1550 emu/cm³. The rougher sample shows some increase in the remanent moment and coercivity, but little change in the saturation field or moment. The larger remanent moment would be expected to decrease the GMR, yet the GMR is much larger in the rougher film. This indicates that the changes in $\Delta R/R$ are not simply due to changes in the fraction of the film coupled antiferromagnetically. On the contrary, the increase in $\Delta R/R$ is so robust as to win out over the decrease in antiferromagnetically coupled regions.

High angle x-ray scans show the films to be bcc [110] oriented, with no other orientations detectable. The peak widths gave typical grain sizes of 100-120Å, and typical rocking curves yielded mosaic spreads of 8-10 degrees. The high angle spectra were only slightly affected by sputtering pressure in agreement with the experimental claims of Takanashi, et al.²⁷ We would like to stress, however, that large effects are observed in the low angle spectra, and only very small changes in the high angle spectra.

Figure 2a shows the CEMS spectra for two $[\text{Fe}(15\text{\AA})/\text{Cr}(15\text{\AA})]_{40}$, one sputtered at 3 mTorr and the other at 12 mTorr. The Fe was chosen to be thinner for the CEMS study to increase the relative contribution of the interfaces. The solid lines are results of fitting the CEMS spectra to a distribution of hyperfine fields. The fit shows that the Fe moments are in-plane, as expected. Fig. 2b shows the hyperfine field distribution for the two samples. The distribution is normalized such that the sum of all the $P(H_N)$ equals one. They are almost identical. The hyperfine field distribution is strongly peaked at the bulk Fe hyperfine field of 330kG and has a tail at lower fields resulting from Fe atoms with Cr atoms in its local environment. For an atomically smooth interface, the two atomic planes closest to the interface will have Cr nearest and next nearest neighbors and thus a reduced hyperfine field. The Fe

layer thicknesses are ≈ 7 monolayers, so only $\approx 3/7^{\text{th}}$ or 43% of the Fe atoms should have the bulk hyperfine field. This is consistent with the height of the $P(H_N=330\text{kG})$ peak heights of 41% and 36% for the 3 and 12 mTorr samples respectively. It is expected that for a rougher interface, there should be a slightly reduced contribution of Fe atoms with the bulk hyperfine field as seen in Fig. 2b. The relatively small changes in the spectra indicate that there is limited interdiffusion which does not change with sputtering gas pressure. The interfacial roughness is increased without appreciably affecting the chemical sharpness of the interface.

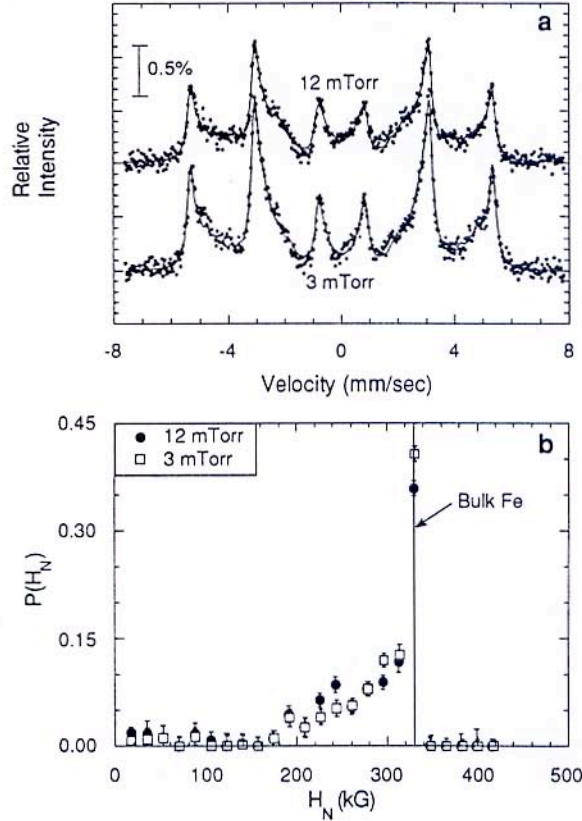


Figure 2: (a) CEMS spectra (solid circles) and fits (lines) for $[\text{Fe}(15\text{\AA})/\text{Cr}(15\text{\AA})]_{40}$ films sputtered at 3 mTorr and 12 mTorr. (b) Distribution of hyperfine fields $P(H_N)$ vs. hyperfine field H_N for spectra shown in (a).

Fig. 3a shows saturation resistivity, ρ_{SAT} , for a series of $[\text{Fe}(30\text{\AA})/\text{Cr}(t_{\text{Cr}})]_{40}$ films. For each argon pressure, the films were grown consecutively to minimize variations in other parameters from sample to sample. The resistivity increases steadily with increasing argon sputtering gas pressure at all Cr thicknesses. Also, the resistivity increases with increasing Cr thickness for all argon pressures, indicating that scattering in the bulk is still the dominant scattering mechanism. In contrast to the 10 bilayer films, the saturation resistivities of the higher pressure films are significantly larger than the low pressure films. Disorder in the films, both interfacial and crystalline, is clearly increasing with increasing number of layers. We would like to stress that the increase of resistance is not due to increases in alloying of Fe and Cr in the bulk or at the interface. This possibility was conclusively ruled out from the CEMS

data presented above. From the x-ray data, the interfaces are clearly becoming much rougher and the crystalline disorder is increasing when the pressure is increased. Interdiffusion in the bulk and at the interface, however, is remaining much the same.

Fig. 3b shows the change in resistivity, $\Delta\rho$, in the same films. This change in resistivity is due to spin dependent scattering of electrons in the material, and it is of great interest to separate it from the resistivity. Generally, the rougher films show an increased $\Delta\rho$ at all Cr thicknesses, and this trend seems strongest at Cr thicknesses above 18 Å. At the lower Cr thicknesses it is expected that some regions in the Fe layers would occasionally ferromagnetically short if the films are rough enough. Therefore, rough films at lower Cr thicknesses would be expected to have less regions of AF coupling and hence smaller enhancement of $\Delta\rho$. This is, in fact, what is observed.

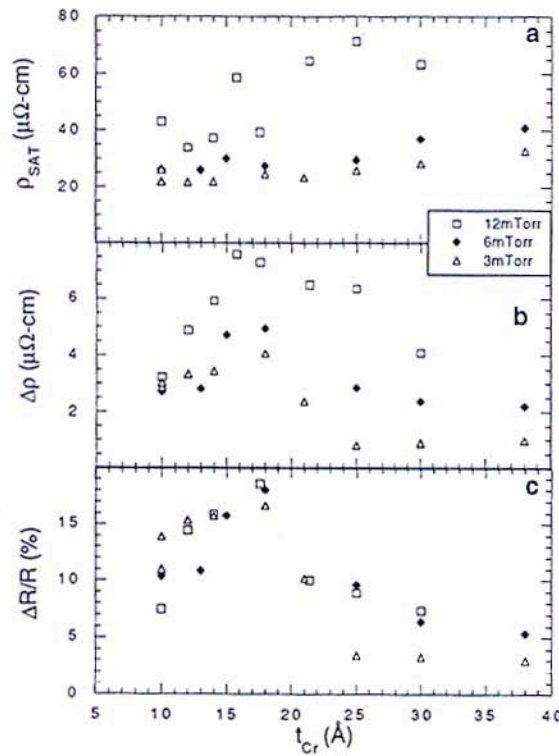


Figure 3: (a) Saturation resistivity ρ_{sat} , (b) change in resistivity $\Delta\rho$, and (c) $\Delta R/R$ for several series of $[\text{Fe}(30\text{\AA})/\text{Cr}(t_{\text{Cr}})]_{40}$ films vs. t_{Cr} sputtered at different pressures. All measurements at 4.2K.

Fig 3c shows the magnetoresistance $\Delta R/R$ for the same films. The $\Delta R/R$ value in general is enhanced with increasing argon pressure. In the roughest samples, $\Delta R/R$ is lower than in the smoother samples at low Cr thicknesses. As mentioned above, a reduced $\Delta\rho$ is expected for the thinner Cr interlayers. Additionally, the saturation resistivity is significantly greater than in the films sputtered at low pressure. These facts both lower the $\Delta R/R$ value. It is important to note that an inspection of $\Delta R/R$ is not sufficient to make comparisons between different samples for this reason. The absolute resistivities are essential in order to obtain a complete characterization of the phenomena of giant magnetoresistance.

In conclusion, we have performed a systematic study of the structure and magnetotransport properties of sputtered Fe/Cr superlattices. By increasing the Ar sputtering pressure, we are able to systematically increase the interfacial roughness of the multilayers. Mössbauer results indicate interdiffusion in the samples is remaining constant with increasing roughness. The spin dependent scattering, $\Delta\rho$, increases with increasing interfacial roughness however the saturation resistivity may also be enhanced by increasing roughness. Thus, the $\Delta R/R$ is not always enhanced by the increase in the $\Delta\rho$. This implies that both ρ_{SAT} and $\Delta\rho$ must be determined separately in order to characterize the magnetotransport properties of Fe/Cr multilayers. Our results demonstrate that interfacial roughness must be a crucial element in any theoretical treatment of giant magnetoresistance in Fe/Cr, and is of great importance to experimentalists in the interpretation of their results.

Work supported by ONR grant No. N00014-91J-1177 (DMK), US DOE grant No. DE-FG03-87ER45332 (EEF, JG, IKS), NSF Grant # DMR-90-10908 (FTP) and grant No. 88/93-130 of the Belgian Concerted Action, G.O.A., and Interuniversity Attraction Poles, IUAP, Programs (YB). International travel was provided by NATO. Some international travel (JG) was provided by a fellowship from CONICET, Argentina. J. Guimpel is on leave from Centro Atómico Bariloche (8400) Bariloche, Rio Negro, Argentina.

References

- 1 M. N. Baibich, J. M. Broto, A. Fert, F. Nguyen Van Dau, F. Petroff, P. Etienne, B. Creuzet, A. Friederich, and J. Chazelas, *Phys. Rev. Lett.* **61**, 2472 (1988).
- 2 J.J. Krebs, P. Lubitz, A. Chaiken, and G.A. Prinz, *Phys. Rev. Lett.* **63**, 1645 (1989).
- 3 A. Barthélémy, A. Fert, M. N. Baibich, S. Hadjoudj, F. Petroff, P. Etienne, R. Cabanel, S. Lequien, F. Nguyen Van Dau, and G. Creuzet, *J. Appl. Phys.* **67**, 5908 (1990).
- 4 S.S.P. Parkin, N. More, and K.P. Roche, *Phys. Rev. Lett.* **64**, 2304 (1990).
- 5 S. Araki and T. Shinjo, *Jpn. J. Appl. Phys.* **29**, L621 (1990).
- 6 G. Binasch, P. Grünberg, F. Saurenbach, and W. Zinn, *Phys. Rev. B* **39**, 4828 (1989).
- 7 B. Dieny, V.S. Speriosu, S.S.P. Parkin, B. A. Gurney, D. R. Wilhoit, and D. Mauri, *Phys. Rev. B* **43**, 1297 (1991).
- 8 P.M. Levy, S. Zhang, and A. Fert, *Phys. Rev. Lett.* **65**, 1643 (1990).
- 9 R. E. Camley and J. Barnás, *Phys. Rev. Lett.* **63**, 664 (1989).
- 10 N. García and A. Hernando, *J. Mag. Mag. Mat.* **99**, L12 (1991).
- 11 J. Inoue, A. Oguri, and S. Maekawa, *J. Phys. Soc. Japan* **60**, 376 (1991).
- 12 P. Grünberg, R. Schreiber, Y. Pang, M.B. Brodsky, and H. Sowers, *Phys. Rev. Lett.* **57**, 2422 (1986).
- 13 P. Baumgart, B. A. Gurney, D. R. Wilhoit, T. Nguyen, B. Dieny, and V. S. Speriosu, *J. Appl. Phys.* **69**, 4792 (1991).
- 14 V. S. Speriosu, B. Dieny, P. Humbert, B. A. Gurney, H. Lefakis, *Phys. Rev. B* **44**, 5358 (1991).
- 15 B. Dieny, P. Humbert, V.S. Speriosu, S. Metin, B. A. Gurney, P. Baumgart, and H. Lefakis, *Phys. Rev. B* **45**, 1297 (1991).
- 16 A. E. Berkowitz, J. R. Mitchell, M. J. Carey, A. P. Young, S. Zhang, F. E. Spada, F. T. Parker, A. Hutten, and G. Thomas, *Phys. Rev. Lett.* **68**, 3745 (1992).
- 17 J. Q. Xiao, J. S. Jiang, C. L. Chien, *Phys. Rev. Lett.* **68**, 3749 (1992).
- 18 F. Petroff, A. Barthélémy, A. Hamzic, A. Fert, P. Etienne, S. Lequien, G. Creuzet, *J. Mag. Mag. Mat.* **93**, 95 (1991).
- 19 I. K. Schuller, *Phys. Rev. Lett.* **44**, 1597 (1980).
- 20 E.E. Fullerton, D. M. Kelly, J. Guimpel, I. K. Schuller, Y. Bruynseraede, *Phys. Rev. Lett.* **68**, 859 (1992).
- 21 E.E. Fullerton, I.K. Schuller, H. Vanderstraeten, Y. Bruynseraede, *Phys. Rev. B* **45**, 9292 (1992).
- 22 F. T. Parker, H. Oesterreicher, E. E. Fullerton, *J. Appl. Phys.* **66**, 5988 (1989).
- 23 K. Takanashi, H. Fujimori, H. Watanabe, M. Shoji and A. Nagai, *Proc. MRS Int'l Mtg. Adv. Mat.* **10**, 397 (1989).
- 24 H. Nagata and S. Seki, *Jpn. J. Appl. Phys.* **29**, 569 (1990).
- 25 D. E. Savage, J. Kleiner, N. Schimke, Y.-H. Phang, T. Jankowski, J. Jacobs, R. Kariotis, M. G. Lagally, *J. Appl. Phys.* **69**, 1411, (1991); S. K. Sinha, *Physica B* **173**, 25 (1991).
- 26 D. L. Windt, R. Hull, K. Waskiewicz, *J. Appl. Phys.* **71**, 2675 (1992).
- 27 K. Takanashi, Y. Obi, Y. Mitani, H. Fujimori, *J. Phys. Soc. Jpn.* **61**, 1169 (1992).